frontiers | Frontiers in Sustainable Food Systems

TYPE Original Research
PUBLISHED 13 July 2023
DOI 10.3389/fsufs.2023.1225792

Check for updates

Performance evaluation and optimization of simultaneous phosphorus and nitrogen removal from anaerobically digested liquid-dairy-manure using an intermittently-aerated-extended-idle sequencing batch reactor

Sehrish Asghar[1], Lide Chen[2]* and B. Brian He[3]

[1]Environmental Science Program, College of Natural Resources, University of Idaho, Moscow, ID, United States, [2]Department of Soil and Water Systems, Twin Falls Research and Extension Center, University of Idaho, Twin Falls, ID, United States, [3]Department of Chemical and Biological Engineering, University of Idaho, Moscow, ID, United States

Wastewater from confined dairy operations requires efficient treatment to reduce its potential to pollute the surrounding environments. In this study, a novel intermittently-aerated-extended-idle sequencing batch reactor (IA-EI SBR) process was developed, evaluated, and optimized for simultaneously removing phosphorus (P) and nitrogen (N) from anaerobically digested liquid-dairy-manure (ADLDM) with lower carbon-to-nutrient-ratios. Four influential operating parameters including cycle-time of 5–9 h, intermittent-aeration strategy of 10–50 min/h, two feed-phases of 6–30 min, and idle-phase of 40–120 min were statistically analyzed using central-composite design coupled with response-surface methodology for optimal removal efficiencies of ortho-phosphorus ($\%OP_{removal}$), total-phosphorus ($\%TP_{removal}$), ammonia-nitrogen ($\%NH_3\text{-}N_{removal}$), total-nitrogen ($\%TN_{removal}$), and chemical oxygen demand ($\%COD_{removal}$). Results showed that the interactions of cycle time-idle phase, and aeration strategy-feed phases were significant in affecting $\%TP_{removal}$ (p-value $\leq$ 0.005). The synergistic effect of aeration strategy-idle phase was significant for $\%TN_{removal}$ and $\%COD_{removal}$ (p-value $\leq$ 0.006), while the cycle time-feed phases interaction had significant effect on $\%NH_3\text{-}N_{removal}$. The maximum simultaneous nitrification-denitrification (SND) efficiency of 85.7% was recorded under influent COD and TN loading of 3,999.2 and 785.7 mg L^{-1} at 30 min/h aeration time in 7 h. The quadratic regression models based on statistical analysis of the experimental results adequately described the IA-EI SBR performance and showed that the applied levels of operating parameters were highly correlated with all five responses (p-value $\leq$ 0.030). Operating conditions for optimal IA-EI SBR process efficiency determined by desirability analysis were cycle-time of 8 h, intermittent-aeration strategy of 36 min/h, feed-phases of 24 min, and idle-phase of 100 min.

OPEN ACCESS

EDITED BY
Umair Ali Toor,
King Abdullah University of Science and Technology, Saudi Arabia

REVIEWED BY
Awais Bokhari,
Comsats University Islamabad, Lahore Campus, Pakistan
Sidra Saqib,
Washington State University, United States

*CORRESPONDENCE
Lide Chen
✉ lchen@uidaho.edu

RECEIVED 19 May 2023
ACCEPTED 26 June 2023
PUBLISHED 13 July 2023

CITATION
Asghar S, Chen L and He BB (2023) Performance evaluation and optimization of simultaneous phosphorus and nitrogen removal from anaerobically digested liquid-dairy-manure using an intermittently-aerated-extended-idle sequencing batch reactor. *Front. Sustain. Food Syst.* 7:1225792. doi: 10.3389/fsufs.2023.1225792

Under these optimal conditions, the corresponding removal efficiencies for OP, TP, NH_3-N, TN, and COD of 82.64, 95.82, 92.92, 73.84, and 90.94%, respectively, were achieved in validation experiments.

KEYWORDS

simultaneous nitrogen and phosphorus removal, sequencing batch reactor, intermittent aeration, extended idle phase, central composite design

1. Introduction

The dairy industry has responded well to the demands for quality meat and milk and promoted rural economic development (Hawkes and Ruel, 2006). Meanwhile, it also creates a large volume of liquid manure containing excessive nutrients from confined dairy operations (Wang et al., 2020b), which are responsible for severe environmental concerns including disruption of the natural nitrogen (N) and phosphorus (P) cycles in adjacent soil and aquatic ecosystems (Filip and Middlebrooks, 1976; Carpenter et al., 1998). According to the U.S. Environmental Protection Agency (EPA), nutrient pollution is one of America's most prevalent, cost-intensive, and demanding environmental issues triggered by N and P runoffs from direct land applications of manure ("The Issue | US EPA, n.d."). The P-runoff from undue land application of manure alone accounts for about 66% of impaired conditions of U.S. rivers (New Patented Technology Removes Phosphorus from Manure, 2018), while the emission of nitrous oxide (N_2O) is another environmental concern as its global warming potential is 265 times of CO_2 (Understanding Global Warming Potentials | US EPA, 2022). Therefore, wastewater from confined dairy operations must be treated satisfactorily by appropriate methods to reduce its polluting potential to the environment. For example, commercial dairy farms in southern Idaho manage manure wastewater onsite adequately through anaerobic biological treatments combined with solid-liquid separation techniques such as screening and centrifugation, which significantly reduce the chemical oxygen demand (COD) and suspended solids (Wang et al., 2020a,b). Still, these treatments generate anaerobically digested (AD) effluents that contain large quantities of P, N, and organic carbon. Thus, it is crucial to employ more efficient biological methods to achieve substantial nutrient reductions.

Biological nutrient removal (BNR) in sequencing batch reactor (SBR) is a promising technology that treats excessive N and P in liquid waste streams, if the synergetic effect of feeding nutrient distribution and aeration intervals is properly managed for best performances. Conventional BNR has been effectively implemented to treat dairy wastewater using single sludge processes in SBR, including anaerobic/anoxic/aerobic (Marañón et al., 2008), and anoxic/aerobic (Castrillón et al., 2009). The basic mechanisms behind BNR processes reveal that satisfactory nutrient removal efficiencies and operational stability of wastewater treatment are associated with high COD to TN ratios (Ferrentino et al., 2016; Barnard et al., 2017).

In conventional BNR, ordinary heterotrophs compete with phosphate accumulating organisms (PAOs) for organic carbon sources, while microbial communities including aerobic heterotrophs, ammonia oxidizing bacteria (AOB), nitrite oxidizing bacteria (NOB), PAO, compete for dissolved oxygen (DO) to removal P and N simultaneously (Wang et al., 2018; Yuan et al., 2020). Thus, inapt operating conditions of SBR or low COD concentration in influents can lead to deterioration of BNR process. Moreover, these processes also encounter difficulties like contrasting sludge retention times (SRTs) and adverse effects of nitrate overaccumulation on functioning microbial consortia (Dai et al., 2021). Researchers have attempted to address the carbon deficiency in BNR processes by adding external carbon sources like ethanol, methanol, and acetic acid (Lee et al., 2001; Louzeiro et al., 2002; Kargi and Uygur, 2003), or by recycling internal carbon sources (Zhang et al., 2013). Clearly, these strategies have major disadvantages such as additional costs for chemicals and energy required for sludge pumping, along with unavoidable greenhouse gas emissions (Caniani et al., 2015; Liu et al., 2021).

In recent years, modern approaches such as partial denitrification, anammox-biological P removal fermentation and partial nitrification (PDA-PFPN) (Fan et al., 2022), combined anammox and denitrifying P removal (CA-DP) (Zhang et al., 2018), denitrifying phosphorus removal and partial nitrification, anammox (DPR-PNA) (Zhang X. et al., 2021), and simultaneous nitrification-denitrification and P removal (SNDPR) (Zeng et al., 2003; Li et al., 2019; He et al., 2020) have been designed to confront the mentioned above challenges and treat wastewaters. Though these approaches have certain advantages such as anammox requires no carbon; but also disadvantages such as extended start-up to establish complex operating schemes, which are often tricky to manage while treating real wastewater. Thus, a simpler SBR scheme is required to efficiently treat ADLDM holding low C: N:P ratios.

In this study, a new scheme, i.e., intermittently aerated-extended idle (IA-EI SBR), has been developed from the aerobic-extended idle (A-EI) SBR and intermittently aerated (IA) SBR (Yoo et al., 1999; Izadi et al., 2021), and adapted to resolve the above-mentioned issues by achieving SNDPR from the anaerobically digested liquid dairy manure (ADLDM) with low C:N:P ratios. The IA-EI SBR is repeatedly alternated between anaerobic, oxic, and anoxic conditions during the entire course of the cycle, followed by settling, decant and an extended idle phase. The concept behind IA-EI SBR is as follows: the biodegradable COD is slowly hydrolyzed into volatile fatty acids (VFAs) which are then taken by denitrifying polyphosphates accumulating organisms (DPAOs) as carbon polymer under anaerobic phase. Subsequently, the shorter aeration time at optimal DO levels prompts the controlled nitrification to maintain nitrates (NO_3-N) in the system, followed by P-absorption by DPAOs using NO_3-N as electron acceptor, under hypoxic or anoxic conditions (Leonard et al., 2018; Dai et al., 2021). The intermittent aeration strategy also restricts competing heterotrophs and improves bioreactor performance. Compared to PAOs in conventional BNR in SBRs, the proliferation of the DPAOs in an optimized bioreactor could lower oxygen and carbon requirements up to 30% and 50%, respectively, along with a 50% reduction in sludge production (Kuba et al., 1996; Chen et al., 2011). The extended-idle phase improves the treatment process similar to A-EI systems, through reducing PAOs dependency on VFAs and increasing the tolerance of higher NO_3^- concentration in the system (Wang et al., 2008, 2012). Fan et al. (2022) also reported stable denitrifying P removal in a novel PDA-PFPN bioreactor with extended idle phase (540 min), while treating domestic wastewater. Because the idle phase is not aerated nor mixed, it also reduces the energy input to the system. The existence and steadiness of biological processes, including P uptake, P release, nitrification, and denitrification, have been indicated by the removals of COD, N and P under specific settings (Wu et al., 2015).

In addition to type of bioreactor, the performance of SNDPR process depends upon operating conditions, i.e., influent COD: N:P ratio, DO and aeration strategy, sludge age, electron acceptors for DPAOs, and HRT (Wu et al., 2023). DO concentrations ranging between 0.05 and 2 mg L^{-1} have been reported optimal for successful SNDPR process (Wu et al., 2023). Whereas the influence of C:N ratio on SNDPR has been found considerably inconsistent in literature, for example, (Liu et al., 2018) reported 84.6% and 55.9% P and N removal while treating municipal wastewater containing C: N of 3.3. Matinfar et al. (2019) studied simultaneous nutrient removal in low-O_2 granular SBR and achieved 97.6 and 97.9% P and N removal from dairy wastewater at C:N ratio of 6.8. Wang et al. (2018) investigated effect of different C:N ratio on SNDPR, and observed decline in denitrification, but consistent COD and P removals in an aerobic granular sludge. Therefore, linking DO, C/N ratio to operating parameters and nutrient removal efficiencies is necessary in achieving better SNDPR performance.

Previous studies have used a single factor approach to evaluate the effects of operating parameters on nutrient removal from diverse forms of wastewaters in SBRs (Lochmatter et al., 2013; Shen et al., 2019; Dan et al., 2020). The optimization approach of "one-factor at a time" often leads to misinterpretations of data, especially when the interaction effects from other operating parameters are not considered in the data analysis. Meanwhile, the central composite design (CCD) coupled with response surface methodology (RSM) allows the assessment of multiple operating parameters at distinct levels in a single design space, thus can be used to analyze the linear and interactive effects of operating parameters and responses more efficiently (Anderson and Whitcomb, 2017a). Therefore, CCD-RSM is a great tool to optimize the distinct phases and evaluate their interactive effects on SNDPR from ADLDM in a novel IA-EI SBR.

The aim of this work was to generate the knowledge of linear and interactive effects of the basic operating parameters including IA, idle phase, feed phases and cycle time on the SNDPR process in the IA-EI SBR for the selection of an efficient treatment of ADLDM containing lower C: N and C:P ratios. The specific objectives were to (i) systematically investigate the collaborative effects of cycle time, aeration time/ strategy, feed phase and extended idle phase on nutrient removal efficiencies, (ii) identify and validate the operating conditions to achieve an optimal performance of the IA-EI SBR, and (iii) develop empirical models based on statistical analysis of experimental results to describe the relationship between the four above-mentioned operating parameters and the nutrient removal efficiencies ($\%OP_{removal}$, $\%TP_{removal}$, $\%NH_3\text{-}N_{removal}$, $\%TN_{removal}$ and $\%COD_{removal}$) and to predict the performances of the SNDPR process in the IA-EI SBR.

2. Materials and methods

2.1. Inoculum and feedstock characteristics

In this study, the IA- EI SBR process was inoculated with acclimated sludge taken from a lab-scale two-step fed SBR operation with superior nutrient removal efficiencies (Asghar et al., 2023). The inoculum sample had a total solid content of 5,500 mg L^{-1}, a volatile suspended solid content of 4,300 mg L^{-1}, and pH of 7.45 ± 0.02. AADLM samples were collected from a centrifugation facility at a commercial dairy in Idaho, kept at 4°C in a refrigerator and used as the substrate in this study. The properties of feedstock tested in this study are summarized in Table 1. The average C: N and C:P ratios of the feedstock were 6:1 and 16:1, respectively, which are considerably lower than recommended limits (Table 6) to support autotrophic and heterotrophic microbial populations and maintain an effective bioreactor (Rollemberg et al., 2019; Zhang et al., 2022).

2.2. IA-EI SBR design and startup

The lab scale SBR was constructed using a clear PVC cylinder (φ25.2 × 50.8 cm D × H) with a total volume of 25 L and a working volume of 20 L. The SBR was equipped with control mechanisms

TABLE 1 Characteristics of feedstock tested in this study.

Parameters	Feedstock
Chemical oxygen demand (mg L^{-1})	4,083 ± 191
Total volatile fatty acid as acetate (mg L^{-1})	1,897 ± 171
Ammonia nitrogen (mg L^{-1})	394 ± 67
Total Kjeldahl nitrogen (mg L^{-1})	469 ± 67
Total nitrogen (mg L^{-1})	720 ± 103
Total phosphorus (mg L^{-1})	261 ± 25
Orthophosphate (mg L^{-1})	113 ± 11
pH	7.32 ± 0.03
COD:TN ratio (mg COD / mg N)	∼6:1
COD:TP (mg COD /mg P)	∼16:1
COD:TN:TP (mg COD / mg N /mg P)	∼16:3:1
OP:TP (mg OP /mg TP)	0.432
NH_3-N:TN (mg NH_3-N /mg TN)	0.547

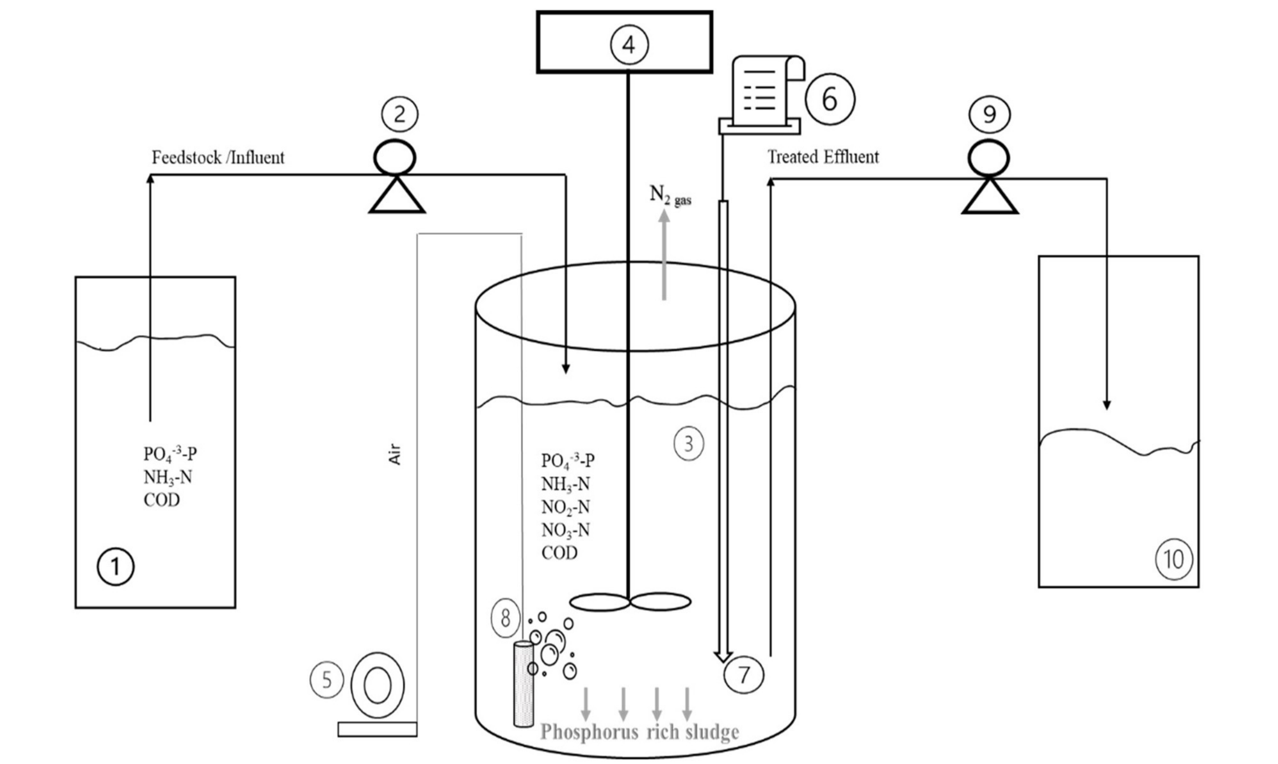

FIGURE 1
Schematic diagram of the IA-EI SBR used in this study. (1) Feedstock/Influent tank; (2) and (9) Peristaltic pumps; (3) Sequencing batch reactor; (4) Mixer on timer; (5) Air pump on timer; (6) LabQuest 2- a data logger; (7) DO and pH probes; (8) Diffusion stone; (10) Effluent tank.

for agitation, aeration, and feeding/discharging (Figure 1). Two peristaltic pumps (Master Flex L/S 7523-90, Cole-Palmer, Vernon Hills, IL, USA) were used to maintain the desired inflow and discharge of ADLDM. A mechanical overhead stirrer (IKA works Inc. Wilmington, NC, USA) was used to provide mixing and controlled via a timer. An agitation speed of 200 rpm was kept during each cycle except settling (40 min), decant (20 min) and idle phase (variable time). An air pump (Tetra, Blacksburg, VA, USA) connected to a gas-diffusion stone (Vivosun, Canada) was used to intermittently aerate the system and regulated by a timer. The aeration pump was set at a 2-min duty period followed by a 2-min quiescent period to maintain the DO concentration of less than 2.5 mg L^{-1} in the system, and to reduce the froth formation. The volume loss in the SBR due to sampling and solids removal was made up with tap water. The pH and DO were monitored using a tris-compatible flat pH sensor and an optical DO probe, linked to a data logger (LabQuest2, Vernier, Beaverton, OR, USA) for data acquisition. The IA-EI SBR was operated at 21-days SRT by maintaining total suspended solids and volatile suspended solids at 0.6–0.8% and 4,240–4,850 mg L^{-1} respectively in the reactor; and 72 h HRT i.e., 6.66 L of wastewater was exchanged daily to the 20 L working volume. The shorter HRTs with high N and P loading rates in system hinders the effective nutrient removal while treating dairy manure wastewater (Matinfar et al., 2019), thus HRT of 72 h was maintained. The cycle time (5–9 h), intermittent aeration strategy (10–30 min/h), feeding duration (6–30 min), and the idle phase (40–120 min) in each experiment were set according to the experimental design as discussed in Section 2.4. The average organic and nitrogen loading rates were 1.347 ± 0.063 kg COD $m^{-3}.day^{-1}$ and 0.238 ± 0.034 kg N $m^{-3}.day^{-1}$ respectively. The total removal efficiencies of nutrients (i.e., OP, TP, NH_3-N, TN, COD) were determined based on the concentration of nutrients in the influent and effluent.

2.3. Sampling and analytical methods

During the experiments, the influent and effluent samples of 30 ml each were collected at the start and the end of each cycle and split into two halves (15 ml each) for testing. The methods developed by the Hach Company (Loveland, CO, USA) were used in the following analytical tests. The first half of the sample was analyzed for COD, total nitrogen (TN), and total phosphorus (TP) using Hach DR5000TM spectrophotometer, based on the methods of reactor digestion (Hach method 8000), persulfate digestion (Hach method 10208), and ascorbic acid (Hach method 10209), respectively. The second half was filtered via a 0.45 µm sterile syringe filter (Tisch Scientific, Cleves, OH, USA) and analyzed for ammonia-nitrogen (NH_3-N) and ortho-phosphate (OP) using the salicylate method (Hach method 10031) and ascorbic acid method (Hach method 10209), respectively. The process intermediates including total volatile fatty acids as acetate (TVFAs), nitrate and nitrite in second half of effluent sample (15 ml) were also

TABLE 2 Experimental range and levels of operating parameters.

Operating parameters		Units	Ranges	Coded levels				
				−α	−1	0	+1	+ α
A	Cycle time	h	5–9	5	6	7	8	9
B	aeration time (the strategy)	min/h	10–50	10 (I)	20 (II)	30 (III)	40 (IV)	50 (V)
C	Two Fill/feed phases	min	6–30	6	12	18	24	30
D	Idle phase	min	40–120	40	60	80	100	120

−α = low axial, +α = high axial, −1 = low factorial, +1 = high factorial and 0 = Central.

monitored using methods of esterification (Hach method 10240), dimethylphenol (Hach method 10206) and diazotization (Hach method 10207), correspondingly (Hach Company, Loveland, CO). The total solids and volatile suspended solids of the collected samples were estimated using the standard methods by (APHA et al., 2012).

2.4. Equations and calculations

The loading rates of organics and nitrogen were calculated using EQ1 and EQ2 respectively (Li et al., 2016; Dionisi and Rasheed, 2018).

$$\text{Organic loading rate (kg COD m}^{-3}\text{.day}^{-1}) = \frac{Q_{\text{inf}} \times COD_{\text{inf}}}{V \times 1000} \quad (1)$$

Where Q_{inf}: the influent flow rate (m^3.day^{-1}); COD_{inf}: COD concentration in influent (mg·L^{-1}) and V: working volume of the reactor (m^3).

$$\text{Nitrogen loading rate (kg Nm}^{-3}\text{.day}^{-1}) = \frac{Q_{\text{inf}} \times N_{\text{inf}}}{V \times 1000} \quad (2)$$

Q_{inf}: the influent flow rate (m^3.day^{-1}); N_{inf}: Influent ammonia nitrogen concentration (mg·L^{-1}) and V: working volume of the reactor (m^3).

$$\text{SRT (days)} = \frac{\text{TSS}_r \times \text{V}}{\text{TSS}_{\text{bulk}} \times \text{Q}_{\text{ex}} + \text{TSS}_{\text{eff}} \times \text{Q}_{\text{eff}}} \quad (3)$$

In EQ 3, TSS_r: total suspended solids concentration in the reactor (mg L^{-1}); V: working volume (L); TSS_{eff}: TSS_{eff} concentration in the effluent (mg L^{-1}); Q_{eff}: effluent flow rate (L d^{-1}), TSS_{bulk}: TSS concentration in the bulk sample (mg L^{-1}) and Q_{ex}: excess sludge flow rate (L d^{-1}). Q_{ex} was calculated based on 21 days of SRT_{target}.

The removal efficiency (%removal) of each nutrient was calculated using the following equation (EQ4).

$$\text{Removal efficiency (\%)} = \left(\frac{\text{C}_{\text{inf}} - \text{C}_{\text{eff}}}{\text{C}_{\text{inf}}}\right) \times 100 \quad (4)$$

where C_{inf} and C_{eff} represent the influent and effluent concentrations of nutrient, respectively, in mg L^{-1}. Herein, the simultaneous nitrification-denitrification (SND) efficiency was considered equal to loss of total inorganic nitrogen (i.e., sum of ammonia, nitrite, and nitrate) during the treatment process (Cheng et al., 2022). Equation (EQ5) was used to calculate SND efficiency under different operating conditions.

$$\text{SND efficiency (\%)} = \left(\frac{(NH_3 - N_{\text{inf}} + NO_2 - N_{\text{inf}} + NO_3 - N_{\text{inf}}) - (NH_3 - N_{eff} + NO_2 - N_{eff} + NO_3 - N_{eff})}{TIN_{\text{inf}}}\right) \times 100 \quad (5)$$

where TIN_{inf} was concentration of total inorganic nitrogen supplied to IA-EI SBR system.

2.5. Experimental design

In this study, batch experiments based on CCD were conducted. Four operating parameters of cycle time (A, h), aeration time/strategy time (B, min/h), two fill/feed phases (C, min) (namely the first at start of cycle and the second half time into cycle), and idle phase (D, min) were investigated. The ranges and levels of these operating parameters are listed in Table 2. The non-aeration segment was always implemented in the beginning of an hour into each aeration strategy and DO was fixed at 2.5 mg L^{-1} during the aeration time. One of the two feed phases was placed at the beginning of the cycle, while the other was positioned halfway through the cycle. The full factorial CCD-RSM was used to determine the testing levels within given ranges and optimize experimental conditions by using the statistical software of Design Expert (version 13.0.5, Stat Ease, Inc., Minneapolis, MN, USA). A total of 30 × 2 batch experiments, including 16 × 2 runs at factorial, 8 × 2 at axial, and 6 × 2 at central points, were performed. Each run was operated for at least 2 weeks to reach a steady state before collecting data as presented in Table 3. The average removal efficiencies of OP, TP, NH_3-N, TN, and COD were the five response variables, hereafter represented as %$OP_{removal}$, %$TP_{removal}$, %NH_3-$N_{removal}$, %$TN_{removal}$ and %$COD_{removal}$.

After the experimental data were obtained and processed, a second-order equation was used to fit the response data as follows:

$$\begin{aligned}\mathbf{Y} = {} & b_0 + b_1A + b_2B + b_3C + b_4D + b_{12}AB + b_{13}AC + b_{14}AD \\ & + b_{23}BC + b_{24}BD + b_{34}CD + b_{11}A^2 + b_{22}B^2 \\ & + b_{33}C^2 + b_{44}D^2 \end{aligned} \quad (6)$$

where **Y** represents the responses, i.e., %$OP_{removal}$, %$TP_{removal}$, %NH_3-$N_{removal}$, %$TN_{removal}$ and %$COD_{removal}$; and A, B, C, and

10.3389/fsufs.2023.1225792

D symbolize the operating parameters, i.e., cycle time, aeration time/strategy, two fill/feed phases and idle phase, respectively. While b_0 is the intercept or offset term; b_1, b_2, b_3 and b_4 are the linear coefficients; b_{11}, b_{22}, b_{33}, and b_{44} are the squared coefficients; and b_{12}, b_{13}, b_{14}, b_{23}, b_{24}, and b_{34} are the interaction coefficients.

The regression model and statistical significance were also constructed and tested using the analysis of variance (ANOVA) test. The main effect of independent variables was assessed at a specific given point in the design space using the perturbation plots. Three-dimensional surface plots were drawn to demonstrate the main and interactive effects of between two operating parameters while keeping the other at the central level. The Design Expert (version 13.0.5, Stat Ease, Inc., Minneapolis, MN, USA) was employed for the experimental design, data analysis, and graph plotting. The desirability function approach was utilized to determine the optimized operating conditions and predicted the nutrient removal efficiencies, which were also experimentally validated.

3. Results and discussion

3.1. Quadratic models for responses based on CCD-RSM

The quadratic models (EQs 3–7) below were obtained based on the CCD-RSM experimental results.

$$\%OP_{\text{removal}} = 83.58 + 4.35A + 3.06B + 3.03C + 1.65D - 3.66AB + 0.44AC + 0.86AD + 2.9BC$$

TABLE 3 Experimental design and results based on the response surface methodology constructed using the design-expert software.

Run	Experimental conditions				Responses				
	A (h)	B (min/h)	C (min)	D (min)	$\%OP_{removal}$	$\%TP_{removal}$	$\%NH_3\text{-}N_{removal}$	$\%TN_{removal}$	$\%COD_{removal}$
1	7	30 (III)	18	120	83.09 ± 3.58	65.95 ± 2.22	80.81 ± 2.26	84.75 ± 0.66	95.88 ± 1.55
2	6	40 (IV)	12	60	70.16 ± 0.040	64.20 ± 4.16	75.50 ± 4.79	50.25 ± 5.61	92.24 ± 2.72
3	9	30 (III)	18	80	75.78 ± 2.21	69.22 ± 5.35	87.00 ± 3.93	61.47 ± 3.90	87.82 ± 2.96
4	6	20 (II)	12	100	64.62 ± 0.55	71.70 ± 2.04	78.26 ± 2.57	89.97 ± 3.56	85.16 ± 5.66
5	6	40 (IV)	12	100	63.16 ± 2.76	72.55 ± 6.49	91.36 ± 2.73	41.65 ± 5.20	93.32 ± 3.68
6	7	30 (III)	6	80	80.32 ± 5.52	75.77 ± 4.77	97.48 ± 2.73	52.42 ± 3.18	90.65 ± 3.25
7	8	20 (II)	12	60	75.00 ± 2.05	65.51 ± 4.74	67.78 ± 7.09	59.85 ± 7.96	89.87 ± 3.10
8	8	40 (IV)	12	60	72.01 ± 3.13	60.67 ± 3.51	91.71 ± 3.71	72.70 ± 1.99	88.76 ± 3.10
9	7	30 (III)	18	80	88.18 ± 0.74	98.17 ± 1.02	87.09 ± 2.87	66.81 ± 1.56	78.48 ± 8.34
10	7	30 (III)	18	40	63.85 ± 1.94	76.98 ± 2.09	95.20 ± 1.24	87.26 ± 2.93	90.67 ± 4.95
11	7	30 (III)	18	80	83.92 ± 3.20	92.58 ± 0.79	85.21 ± 3.04	62.92 ± 3.58	80.28 ± 2.63
12	7	30 (III)	18	80	86.92 ± 3.82	84.74 ± 0.74	83.93 ± 4.92	60.73 ± 2.62	78.05 ± 8.34
13	7	10 (I)	18	80	63.54 ± 0.81	68.45 ± 4.23	68.85 ± 10.75	65.84 ± 2.52	80.72 ± 4.81
14	8	40 (IV)	12	100	71.81 ± 3.59	73.43 ± 3.80	77.56 ± 5.67	43.19 ± 1.30	93.31 ± 4.38
15	7	30 (III)	30	80	89.40 ± 3.04	94.25 ± 4.23	93.75 ± 1.92	62.55 ± 4.13	91.31 ± 1.70
16	8	20 (II)	24	60	73.57 ± 5.43	71.15 ± 7.50	84.22 ± 4.82	59.42 ± 4.68	86.19 ± 3.39
17	6	40 (IV)	24	100	79.98 ± 6.58	68.98 ± 4.96	69.98 ± 6.58	52.69 ± 1.54	95.71 ± 1.98
18	7	30 (III)	18	80	77.02 ± 2.36	94.82 ± 0.74	90.30 ± 2.90	64.74 ± 2.83	82.09 ± 2.69
19	7	30 (III)	18	80	89.29 ± 0.21	93.73 ± 1.48	89.85 ± 3.56	72.88 ± 3.59	76.66 ± 6.08
20	8	20 (II)	24	100	78.65 ± 4.91	87.61 ± 1.47	88.11 ± 3.49	57.80 ± 1.87	79.90 ± 3.69
21	6	20 (II)	24	60	58.41 ± 6.08	69.11 ± 2.06	68.34 ± 2.01	47.15 ± 2.79	84.13 ± 5.23
22	8	40 (IV)	24	60	75.72 ± 1.16	76.90 ± 2.64	96.34 ± 1.30	79.20 ± 5.67	81.63 ± 2.12
23	8	40 (IV)	24	100	87.54 ± 2.05	98.82 ± 0.64	91.84 ± 1.16	70.34 ± 4.10	91.80 ± 3.56
24	6	20 (II)	24	100	50.45 ± 1.74	62.38 ± 3.39	75.92 ± 1.94	82.40 ± 2.90	80.13 ± 6.02
25	5	30 (III)	18	80	62.29 ± 2.69	71.69 ± 2.49	73.21 ± 3.62	49.35 ± 0.62	77.38 ± 8.06
26	8	20 (II)	12	100	65.79 ± 2.23	77.82 ± 1.88	78.77 ± 8.95	86.88 ± 4.79	87.40 ± 2.21
27	6	40 (IV)	24	60	84.40 ± 3.83	96.20 ± 2.05	75.73 ± 2.33	69.64 ± 2.87	77.32 ± 4.40
28	7	50 (V)	18	80	56.84 ± 4.77	72.91 ± 2.46	87.70 ± 3.08	45.87 ± 3.38	79.64 ± 2.76
29	6	20 (II)	12	60	51.55 ± 2.67	69.39 ± 1.17	83.24 ± 4.84	81.32 ± 4.44	85.55 ± 3.11
30	7	30 (III)	18	80	76.18 ± 4.14	92.18 ± 3.39	78.49 ± 1.48	84.24 ± 3.93	82.68 ± 1.74

A, Cycle time; B, aeration time (the strategy); C, Two Fill/feed phases; D, Idle phase.

$$- 0.048BD + 0.049CD - 3.92A^2 - 2.74B^2 + 0.16C^2 - 2.291D^2 \quad (7)$$

$$\%TP_{\text{removal}} = 92.70 + 1.35A + 1.92B + 4.70C + 0.75D - 1.35AB + 2.39AC + 5.42AD + 4.01BC - 0.53BD - 1.96CD - 5.60A^2 - 5.55B^2 - 1.97C^2 - 5.35D^2 \quad (8)$$

$$\%NH_3 - N_{\text{removal}} = 85.81 + 3.57A + 3.46B - 0.048C - 0.82D + 1.99AB + 5.19AC - 1.03AD + 0.67BC + 1.63BD - 0.40CD - 2.10A^2 - 2.56B^2 + 1.69C^2 - 0.21D^2 \quad (9)$$

$$\%TN_{\text{removal}} = 68.72 + 1.61A - 5.21B + 0.55C + 0.02D + 5.51AB + 0.96AC - 1.96AD + 8.46BC - 8.33BD + 0.64CD - 3.067A^2 - 2.95B^2 - 2.547C^2 + 4.59D^2 \quad (10)$$

$$\%COD_{\text{removal}} = 79.70 + 1.09A + 1.4B - 1.56C + 1.31D - 0.72AB - 0.052AC - 0.57AD - 0.22BC + 2.95BD + 0.97CD + 0.77A^2 + 0.16B^2 + 2.86C^2 + 3.44D^2 \quad (11)$$

The results of ANOVA suggested that the quadratic models are highly statistically significant with low p-values of 0.0007–0.0301 (Table 4). The insignificant lack of fit relative to the pure errors supported the validity of the quadratic models (p-value > 0.05). The coefficients of determination (R^2) of 0.753, 0.847, 0.753, 0.836, and 0.833 for $\%OP_{\text{removal}}$, $\%TP_{\text{removal}}$, $\%NH_3\text{-}N_{\text{removal}}$, $\%TN_{\text{removal}}$ and $\%COD_{\text{removal}}$, respectively, demonstrated excellent correlations between the predicted and experimental results in the experimental domain. The ratio of signal (response) to noise (deviation) is reflected by the predictive precision of the models, which compares the mean error of predictions to the range of predicted values at the design points (Anderson and Whitcomb, 2017b), and a ratio of larger than 4 is desirable (Bilici Baskan and Pala, 2010). Herein, the adequate precision values of 6.71, 6.91, 7.98, 9.66, and 7.08 for $\%OP_{\text{removal}}$, $\%TP_{\text{removal}}$, $\%NH_3\text{-}N_{\text{removal}}$, $\%TN_{\text{removal}}$ and $\%COD_{\text{removal}}$, respectively, verify the appropriate the adequacy of the predicting models. The data fitting potential of the developed polynomial quadratic models is also corroborated by plotting the experimental data against the predicted values for the responses (Figure 2), where the proximity between the model predictions and experimental results was observed. It is concluded that the models derived from CCD-RSM are sufficient to estimate effects of the operating parameters on the nutrient removal efficiencies.

3.2. Effects of operating parameters on nutrient removal efficiencies

Table 3 summarizes the performance of the IA-EI SBR in removing nutrients from ADLDM under different conditions. The efficiencies $\%OP_{\text{removal}}$, $\%TP_{\text{removal}}$, $\%NH_3\text{-}N_{\text{removal}}$, $\%TN_{\text{removal}}$ and $\%COD_{\text{removal}}$ were in the ranges of 50.45–89.44, 60.67–98.82, 67.78–97.48, 41.65–92.70, and 76.66–95.88%, respectively, which suggested that the selected levels of the operating parameters were appropriate because the optimal values of the responses were apprehended effectively from the experimental design.

In this study, increasing the cycle time (variable A) significantly improved the removals of soluble phosphorus and nitrogen (i.e., OP and NH_3-N), whereas $\%TP_{\text{removal}}$, $\%TN_{\text{removal}}$ and $\%COD_{\text{removal}}$ did not show substantial variations to cycle time (p-value > 0.05), suggesting that the microbial consortia did not require only an extended cycle time, but the optimal combination of the operating parameters to generate a favorable environment to maintain an excellent bioreactor performance. The intermittent aeration strategy (variable B) tested in this study impacted the $\%NH_3\text{-}N_{\text{removal}}$ and $\%TN_{\text{removal}}$ significantly (p-value < 0.05), but no significant variations of $\%OP_{\text{removal}}$, $\%TP_{\text{removal}}$ and $\%COD_{\text{removal}}$ were noticed under the linear effect of intermittent aeration strategy. According to the ANOVA analysis, the direct effect of feed phases (variable C) on $\%TP_{\text{removal}}$, and $\%COD_{\text{removal}}$ was found significant (p-value ≤ 0.05). However, the linear effect of idle phase (variable D) was not found statistically significant for all five responses in this study. To further understand the interactive effects of the operating parameters on each response, contour plots and 3D surface response plots were generated by altering two operating parameters within the experimental ranges and keeping the other two at the central level (the coded value of 0).

3.2.1. Ortho-phosphate removal performance

In this study, the superior efficiencies of ortho-phosphate removal ($\%OP_{\text{removal}}$) were achieved at higher levels of residual nitrate/nitrite concentrations in the system (Figure 3), which specifies that the P removal might be dependent on anoxic P uptake in IA-EI SBR. Moreover, the higher P removals in IA-EI process can be maintained under lower influent carbon to phosphorus ratio (16:1) than conventional anaerobic/ aerobic/ anoxic processes. Therefore, the significant P removals observed can be associated to the high P-uptake by denitrifying phosphate accumulating organisms (DPAOs), as previously reported in the literature (Wang et al., 2009; Bassin et al., 2012). The linear effects of cycle time (variable A) and the second-order effect of cycle time (i.e., A^2) and of aeration time/strategy (i.e., variable B^2) were significant for $\%OP_{\text{removal}}$ (p-value < 0.05), but none of the interactions between the operating parameters were significant on $\%OP_{\text{removal}}$ (Table 4). The perturbation plot of $\%OP_{\text{removal}}$ confirms that the cycle time and aeration time/strategy were the most influential parameters, followed by the feed phases and idle phase (Supplementary Figure 1a). The color gradient of response surface plots represents the interactive effect of cycle time and aeration time/strategy on $\%OP_{\text{removal}}$ (Figure 4), where the extended aeration (30–40 min/h) and cycle time (8–9 h) improved the OP removals when the idle phase and feed phases were fixed at 80 and 18 min, respectively. The extended aeration time had supplied adequate electron acceptors (e.g., oxygen, nitrates, and nitrites) in the system for effective P removal. Under these conditions, the DPAOs seem to outcompete the heterotrophic bacteria (non-PAOs), thus promoting P uptake and denitrification simultaneously, evidenced by the higher removal efficiencies of TP and TN along with COD achieved during Runs 23 and 30. DPAOs activity can be maintained in SBR if the concentration of nitrates was sufficient to exceed

TABLE 4 ANOVA results and fit statistics for the quadratic models.

Responses	$\%OP_{removal}$				$\%TP_{removal}$				$\%NH_3\text{-}N_{removal}$				$\%TN_{removal}$				$\%COD_{removal}$			
Source	SS (1)	MS (2)	F-value	p-value	SS (1)	MS (2)	F-value	p-value	SS (1)	MS (2)	F-value	p-value	SS (1)	MS (2)	F-value	p-value	SS (1)	MS (2)	F-value	p-value
Model	2,754.63	196.76	3.27	**0.015**	3,528.91	252.07	5.93	**0.001**	1,607.07	114.79	2.76	**0.030**	4,951.14	353.65	5.45	**0.001**	837.36	59.81	4.38	**0.004**
A-Cycle time	453.62	453.62	7.53	**0.015**	43.90	43.90	1.03	0.326	305.16	305.16	7.34	**0.016**	61.92	61.92	0.96	0.344	28.56	28.56	2.09	0.169
B-Aeration time	224.11	224.11	3.72	0.073	88.17	88.17	2.08	0.170	287.60	287.60	6.92	**0.019**	651.77	651.77	10.05	**0.006**	47.04	47.04	3.44	0.083
C-Feed phases	220.71	220.71	3.66	0.075	530.54	530.54	12.49	**0.003**	0.06	0.06	0.00	0.971	7.14	7.14	0.11	0.745	58.53	58.53	4.28	**0.056**
D-Idle phase	65.54	65.54	1.09	0.313	13.65	13.65	0.32	0.579	16.40	16.40	0.39	0.539	0.01	0.01	0.00	0.993	41.24	41.24	3.02	0.103
A × B	214.62	214.62	3.56	0.079	29.21	29.21	0.69	0.420	63.04	63.04	1.52	0.237	484.99	484.99	7.48	**0.015**	8.24	8.24	0.60	0.450
A × C	3.17	3.17	0.05	0.822	91.30	91.30	2.15	0.163	431.39	431.39	10.38	**0.006**	14.92	14.92	0.23	0.638	0.04	0.04	0.00	0.956
A × D	11.90	11.90	0.20	0.663	470.24	470.24	11.07	**0.005**	16.97	16.97	0.41	0.532	61.27	61.27	0.95	0.346	5.20	5.20	0.38	0.547
B × C	134.44	134.44	2.23	0.156	257.76	257.76	6.07	**0.026**	7.26	7.26	0.17	0.682	1,144.64	1,144.64	17.65	**0.001**	0.78	0.78	0.06	0.814
B × D	0.04	0.04	0.00	0.980	4.56	4.56	0.11	0.748	42.32	42.32	1.02	0.329	1,109.39	1,109.39	17.11	**0.001**	140.07	140.07	10.25	**0.006**
C × D	3.86	3.86	0.06	0.804	61.23	61.23	1.44	0.249	2.64	2.64	0.06	0.804	6.57	6.57	0.10	0.755	15.02	15.02	1.10	0.311
A^2	422.11	422.11	7.01	**0.018**	861.38	861.38	20.28	**0.000**	131.63	131.63	3.17	0.095	257.27	257.27	3.97	0.065	16.17	16.17	1.18	0.294
B^2	1,032.08	1,032.08	17.14	**0.001**	844.17	844.17	19.87	**0.001**	192.34	192.34	4.63	**0.048**	238.92	238.92	3.69	0.074	0.73	0.73	0.05	0.821
C^2	0.03	0.03	0.00	0.982	105.93	105.93	2.49	0.135	78.05	78.05	1.88	0.191	177.50	177.50	2.74	0.119	224.81	224.81	16.45	**0.001**
D^2	217.22	217.22	3.61	0.077	785.50	785.50	18.49	**0.002**	1.28	1.28	0.03	0.863	576.90	576.90	8.90	**0.009**	323.95	323.95	23.70	**0.000**
Residual	903.33	60.22			637.26	42.48			623.35	41.56			972.51	64.83			205.05	13.67		
Lack of Fit	740.50	74.05	2.27	0.189	538.14	53.81	2.71	0.141	527.76	52.78	2.76	0.137	597.36	59.74	0.7962	0.646	176.67	17.67	3.11	0.111
Pure Error	162.83	32.57			99.12	19.82			95.6	19.12			375.14	75.03			28.38	5.68		
Cor Total	3,657.96				4,166.18				2,230.42				5,923.65				1,042.41			
$\mathbf{R^2}$	0.753				0.847				0.720				0.836				0.803			
Adeq precision	6.71				7.98				6.91				9.66				7.08			

(1) SS, sum of squares; (2) MS, mean squares.

The model terms with p-value lower than 0.1 can be considered effective, whereas the terms with p-value lower than 0.05 and **0.001** could be concluded as statistically significant and highly statistically significant, respectively.

10.3389/fsufs.2023.1225792

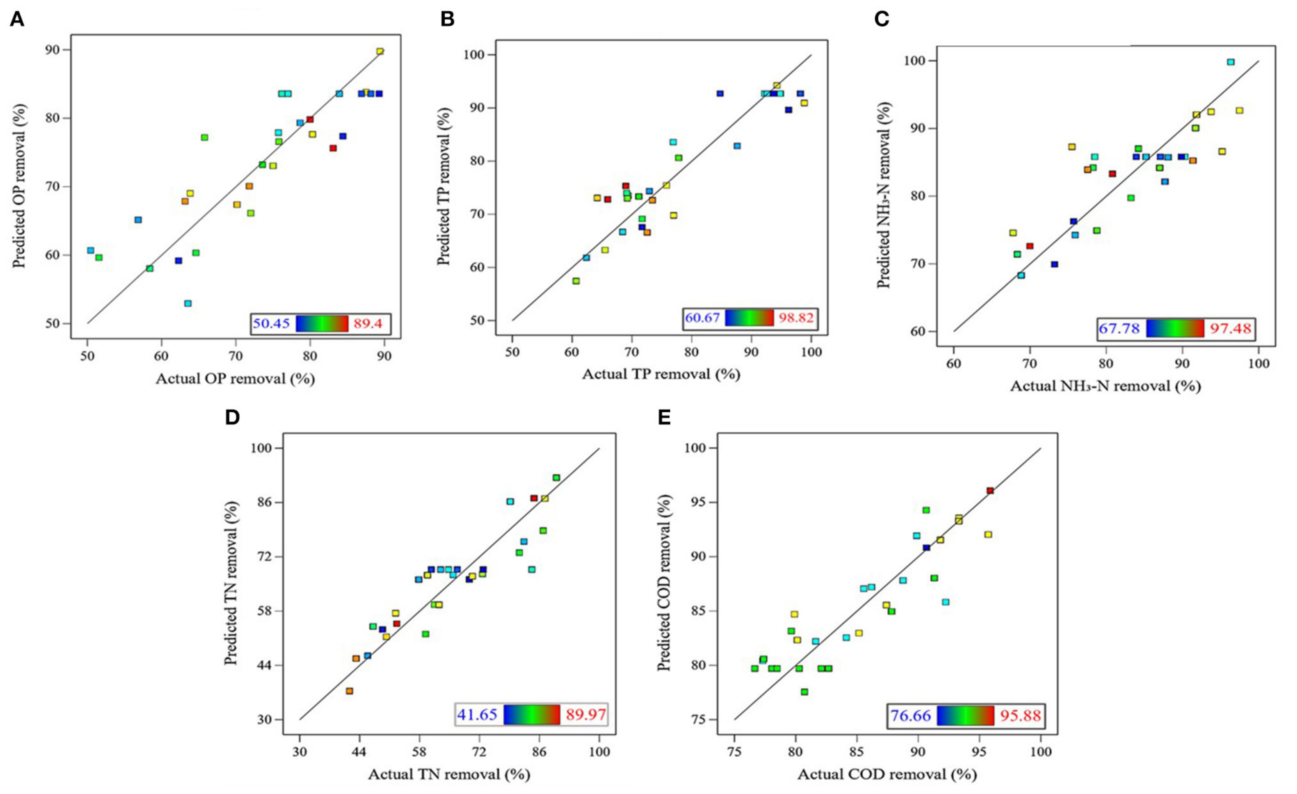

FIGURE 2
Linear correlations between the predicted (line) and experimental data (dots) for **(A)** $\%OP_{removal}$, **(B)** $\%TP_{removal}$ **(B)** a1, **(C)** $\%NH_3\text{-}N_{removal}$, **(D)** $\%TN_{removal}$, **(E)** $\%COD_{removal}$.

the denitrification potential of heterotrophs (Chen et al., 2015; Dai et al., 2022), while rapid variations in aeration time (10–20 min/h) and shorter cycle time (≤ 6 h) negatively affected the $\%OP_{removal}$. In Runs of 24 and 13 (idle phase ≥ 80 min), lower $\%OP_{removal}$ of 50.45% and 63.54%, respectively, were recorded. However, why these aeration strategies did not work well for OP removal despite sufficient time in idle phase for carbon uptake remains unanswered to the authors. Further research is needed to explore the related causing factors and potential mechanisms. As presented in Figure 4B, $\%OP_{removal}$ was improved at feed phases of 24 min or longer and idle phase of 80 min or longer under the fixed cycle time of 7 h and aeration time/strategy of 30 min/h. The high efficiency of $\%OP_{removal}$ recorded in Run 15 suggested that an optimal DPAOs activity was maintained, regardless of higher nitrification under these conditions (Figure 3). Similar trends for $\%TP_{removal}$ were also observed in Runs of 13,15, and 24.

3.2.2. Total phosphorus removal performance

Analyzing the prediction model in EQ 4 revealed that the interactive effects of cycle time and idle phase (A × D) and aeration time/strategy and feed phase (B × C), feed phase and idle phase (C × D) and second-order effects of cycle time (A^2), aeration time/strategy (B^2) and idle phase (D^2), were significant for $\%TP_{removal}$. Also, the steep curves for the feed phases and idle phase in the pertubation plots explain the sensitivity of $\%TP_{removal}$ toward variations between applied levels (Supplementary Figure 1b). These findings are further supported by the reponse surface plots of cycle time and idle phase (A × D), aeration time/ strategy and feed phases (B × C), and feed phases and idle phase (C × D) on $\%TP_{removal}$ as presented in Figure 4. Though, the effect of feed phases on both $\%TP_{removal}$ and $\%COD_{removal}$ was significant (p-value ≤ 0.05), but shorter feed phases (6–12 min) encouraged COD removals, and negatively affected $\%TN_{removal}$ and $\%TP_{removal}$ in this study. The observations in Run 6 suggested that the substantial $\%COD_{removal}$ was achieved by ordinary heterotrophs rather than by DPAOs or denitrifiers under these conditions.

The continuous rise in slope showed that $\%TP_{removal}$ was enhanced with increasing duration of feed and idle phases (Figure 4C). The carbon availability in the IA-EI SBR was well controlled by shifting the feed phases (6 to 18 min), which favored DPAOs as implied by the significant increases in $\%TN_{removal}$ and $\%TP_{removal}$ along with $\%COD_{removal}$ in Runs of 9, 11, 15, 18, and 19. The adequate total VFAs in system due to lengthier feed phases, and extended idle phase (≥ 80 min) appeared to offer ideal anaerobic/anoxic environment for additional carbon uptake as intracellular polymers, which was ultimately utilized for P uptake (Figure 3).

The shorter idle phase combined with longer cycle time clearly exacerbated the P removal evidenced by 76.98% of TP removal in Run 10 (SND = 84.1%), despite of the best feeding and intermittent aeration strategy. The $\%TP_{removal}$ surface plot of aeration time/

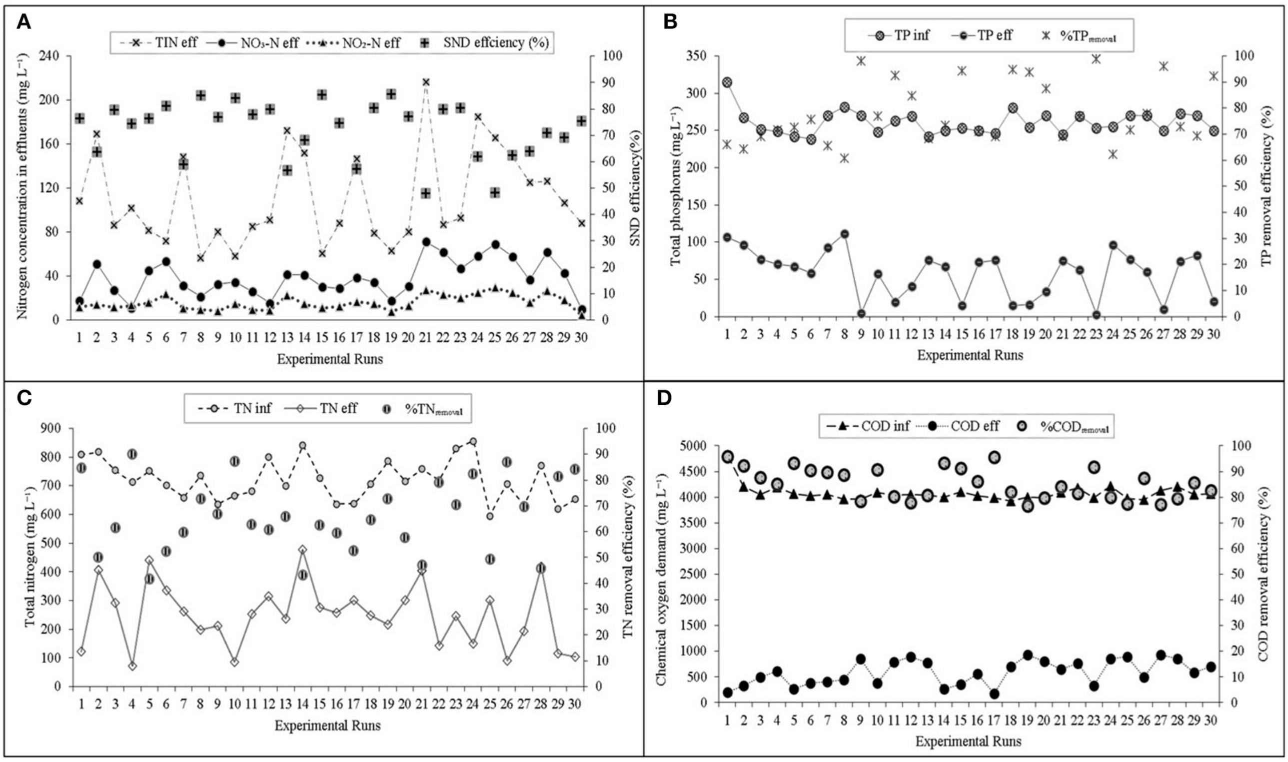

FIGURE 3
Simultaneous C, N and P removal performance in IA-EI SBR under different operating conditions **(A)** TIN and NOx-N variations in effluent and SND efficiency (%) under applied experimental conditions **(B)** $\%TP_{removal}$; **(C)** $\%TN_{removal}$; **(D)** $\%COD_{removal}$.

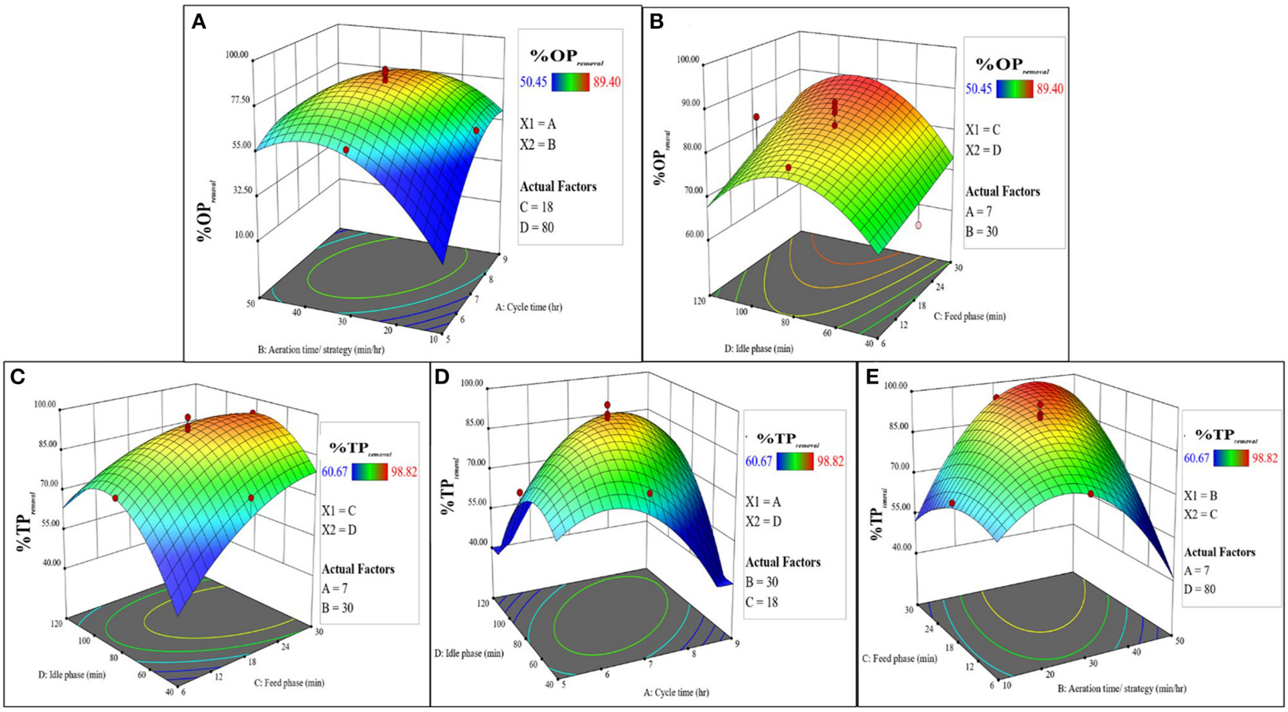

FIGURE 4
Response surface plots for $\%OP_{removal}$ **(A)** cycle time and aeration time/ strategy, **(B)** feed phase and idle phase; $\%TP_{removal}$ against interaction between **(C)** feed phase and idle phase **(D)** cycle time and idle phase, **(E)** aeration time/ strategy and feed phase.

strategy and feed phases (B × C) in Figure 4E suggests that the negative effect of longer aeration time on TP removal can be overturned by changing feed distribution or increasing idle phase. The TN removal exhibited a similar trend under changing duration of feed phases and extended intermittent aeration strategy. These observations elucidate that the IA-EI SBR process provides more operational flexibilities to control the deleterious effects of process intermediates than the conventional biological treatment systems.

3.2.3. Ammonia-nitrogen removal performance

Traditionally, biological NH_3-N removal involves the conversion of ammonia to nitrites and nitrates by ammonia-oxidizing bacteria (AOBs) and nitrite-oxidizing bacteria (NOBs) under aerobic conditions (Ji et al., 2020). Highlighted data in Table 4 indicate that the linear effects of cycle time (A) and aeration time (B), the second-order effect of aeration time (B^2), and the two-level interaction of cycle time and feed phases (A × C) were significant in affecting the %NH_3-$N_{removal}$ (p-value < 0.05). and In the perturbation plot, %NH_3-$N_{removal}$ was found more sensitive to the fluctuating aeration time and cycle time in contrast to the other two parameters (Supplementary Figure 1c). In this study, longer aeration time significantly improved the %NH_3-$N_{removal}$ due to a complete nitrification (p-value = 0.019). Shorter cycle time and feed phases tended to lower ammonia concentration in the effluent faster at 30 min/h of aeration time due to higher nitrification rate (evident by increase in residual nitrates in system), but negatively influenced the overall nutrient removal (Figures 3, 5A). These conditions had led to rapid generation of nitrates, thus disrupting the mandatory balance between nitrification and denitrification, and the P removal processes, which was apparent from the declines in TP and TN removal efficiencies. On the contrary, longer feed phases were observed to escalate the nitrification process by manipulating the availability of NH_3-N to microbes, therefore, controlled production of nitrates and nitrites in the system and ensured the simultaneous removals of P and N at higher rates (Figures 3, 5A). These observations agree with the findings by Mang et al. (2022) on that an optimal step-feed distribution over time improves N and P removal rates through adjusting the C/N ratios in the system. However, the effect of idle phase on nitrification process was negligible, indicated by the flat trajectory in %NH_3-$N_{removal}$ response plot (Figure 5C).

3.2.4. Total nitrogen removal performance

DPAOs consume nitrites and nitrates as electron acceptors under optimal intermittent aeration strategy and remove them from the system as N_2 gas (Zhang M. et al., 2021). In this study, the linear effect of aeration time (B), the interaction effects of cycle time and aeration time/ strategy (A × B), aeration time/ strategy and feed phase (B × C), aeration time/ strategy and idle phase (B × D) and the second-order effect of idle phase (D^2) were significant for %$TN_{removal}$ (p-value < 0.05). Increasing aeration time enhances the DO availability in system and might support aerobic heterotrophs, thus encouraging complete nitrification instead of the DPAOs proliferation, which can result in incomplete denitrification and high N concentrations in the effluent (Raper et al., 2018). Perturbation plots show that all four operating parameters affected removal of total nitrogen. The sensitivity of %$TN_{removal}$ toward variations in operating parameters was ranked as aeration time/strategy > idle phase > cycle time > feed phases (Supplementary Figure 1d).

Further evaluations of interactive relationships between the operating parameters and %$TN_{removal}$ are shown as 3D response surface plots in Figure 5. A negative interactive effect of cycle time and aeration time/strategy can be seen in Figure 5D which confirms that non-aerated phases of 10–20 min/h were insufficient for complete denitrification. These conditions resulted in significantly higher residual concentrations of nitrates and nitrites in effluents of Runs 5 and 28 (Figure 3). Denitrifying bacteria are facultative anaerobes and cannot metabolize the nitrates in the presence of oxygen, complete denitrification only occurs under anoxic conditions and ample substrate (carbon) to maintain their growth (Albina et al., 2019). Figure 5E shows that the negative effects of extended aeration time on %$TN_{removal}$ was annulled by the optimal duration of the feed phases. The TN removal efficiency was substantially enhanced from 43.19% (in Run 14) to 79.20% (in Run 22) by extending the duration feed phase from 12 to 24 min, when influent TN loading were 840.4 and 721.0 mg. L^{-1}, respectively. Interestingly, the maximum and minimum %$TN_{removal}$ of 89.97% and 41.65% were observed in Run 4 (SND = 74.4%; 20 min/h of aeration) and Run 5 (SND = 76.3%; 40 min/h of aeration), with influent TN loading of 752.7 and 712.7 mg.L^{-1}, respectively, while both runs were operated at 6h cycle time, 12 min feed phases and 100 min idle phase. Herein, the combined effect of the idle phase and aeration time on %$TN_{removal}$ was intricate (Figure 5F). The longer idle phase (100 min) coupled with a shorter aeration time (10 min/h) resulted in complete denitrification. In contrast, the runs operated at a shorter idle phase required a longer aeration time ($\geq$ 40 min/h) to achieve lower nitrate concentrations in the effluent. Additionally, the idle phase of 80 min might have positioned heterotrophic PAOs at an advantage over denitrifying bacteria while competing for carbon sources, subsequently leading to a poor TN removal efficiency but steady %$TP_{removal}$ (for instance in Run 6 and 27). It can be concluded that the duration of feed phases is the most critical operating parameter for maximizing the simultaneous removal of TP and TN from low carbon ADLDM.

3.2.5. Chemical oxygen demand removal performance

The quadratic interactions of aeration time/strategy and idle phase (B × D) along with the second order effects of feed phases (C^2) and idle phase (D^2) had a significant impact on %$COD_{removal}$ (p-value < 0.05). The steep curves in the feed phases and idle phase of the perturbation plots suggest an extreme sensitivity of %$COD_{removal}$ toward the change in these variables (Supplementary Figure 1e). Under fixed feed and idle phases at their central levels (namely, 18 and 80 min), the quadratic effect of cycle time and intermittent aeration strategy (A × B) positively influenced %$COD_{removal}$ as seen in Figure 6A. The %$COD_{removal}$ was recorded remarkably low (∼70%) under 10 min/h intermittent aeration strategy and shorter cycle time of 5 h. It was observed that when intermittent aeration and cycle time were both increased from 10 to 30 min/h and from 5 to 7 h, respectively, the average %$COD_{removal}$

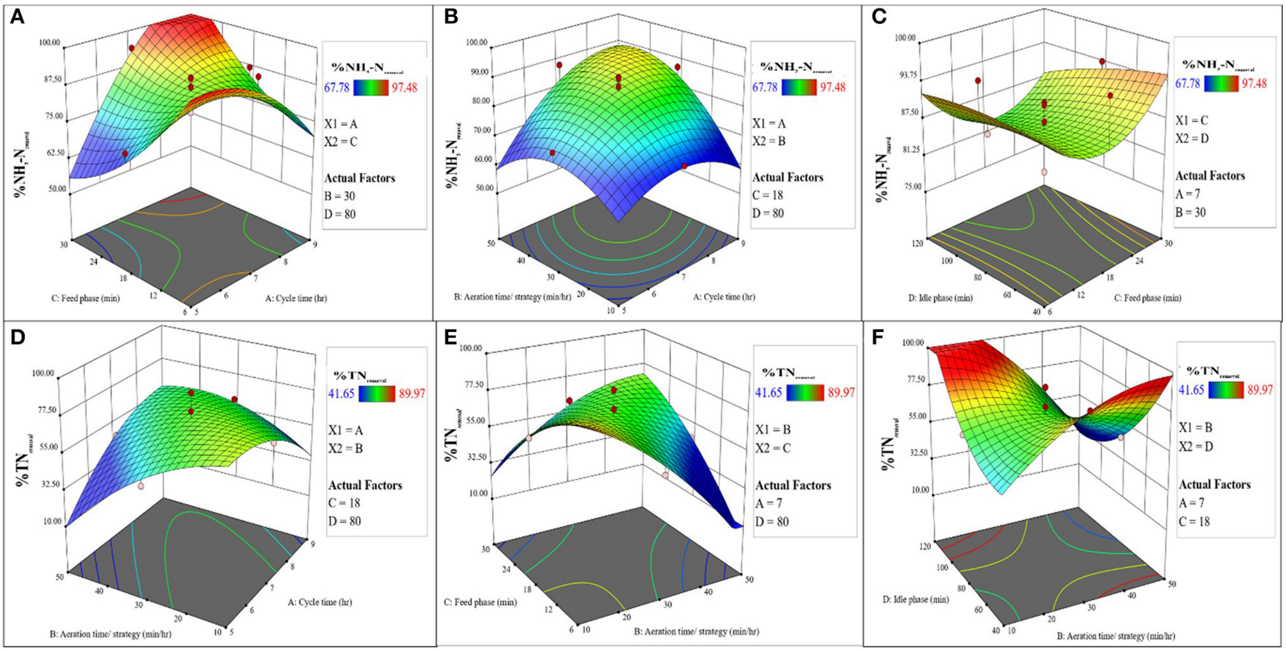

FIGURE 5
Response surface plots for $\%NH_3\text{-}N_{removal}$ against interaction of **(A)** cycle time and feed phases **(B)** cycle time and aeration time/strategy **(C)** feed phases and idle phase; and $\%TN_{removal}$ against interaction of **(D)** aeration time/strategy and cycle time **(E)** Feed phases and aeration time/strategy **(F)** aeration time/strategy and idle phase.

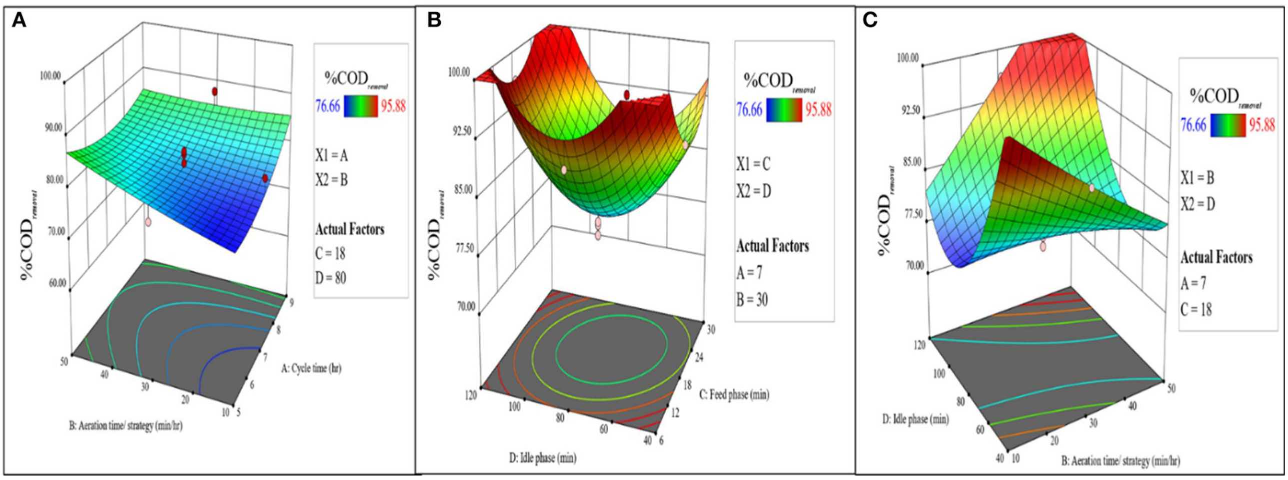

FIGURE 6
Response surface plots for $\%COD_{removal}$ against interaction of **(A)** cycle time and aeration time/strategy **(B)** feed phases and idle phase **(C)** aeration time /strategy and idle phase.

were unchanged. The inadequate reaction time for heterotrophs or DPAOs to metabolize COD, and the lesser consumption of rbCOD for denitrification due to lower NO_3-N and NO_2-N concentrations in the system can be the explanations for these observations (Diez et al., 2002). It has been noted that a shorter intermittent aeration time requires a longer cycle duration to decrease the same quantity of COD or vice versa. The plausible explanation to these observations is that heterotrophs consume organic matter via carbon oxidation under sufficient oxygen availability (Guadie et al., 2014; Hai et al., 2015). Figure 6B represents the significantly enhanced COD removal efficiencies under the interactive effect of idle phase and feed phases at fixed levels of cycle time (7 h) and aeration time (30 min/h). In this study, the shorter feed phases might have favored the selection of ordinary heterotrophs instead of DPAOs in the system, evidenced by superior COD removal efficiency but poor overall P removal under these conditions. Provided that feed volume was kept constant in this study, shorter feed phases can be taken as an

10.3389/fsufs.2023.1225792

TABLE 5 Results of validation experiments.

Response	Predicted values	Experimental results (%) *	Relative error (%)
$\%OP_{removal}$	84.26	82.64	1.96
$\%TP_{removal}$	95.10	95.82	−0.75
$\%\ NH_3\text{-}N_{removal}$	91.90	92.92	−1.10
$\%TN_{removal}$	68.80	73.84	−6.83
$\%COD_{removal}$	89.90	90.94	−1.14

*Averages of two experiments.

alternative for higher organic loading, implying that more rbCOD was readily available to microbes to thrive and metabolize nutrients simultaneously. The interactive effect of aeration time/strategy and idle phase (B × D) in Figure 6C depicts that the increase in levels of these operating parameters significantly improved $\%COD_{removal}$. The maximum $\%COD_{removal}$ of 95.88% was achieved in Run 1 at influent COD of 4821 ± 199 mg L^{-1}, which was operated at an idle phase of 120 min and aeration time of 30 min/h for 7 h.

High removal efficiencies for phosphate, nitrogen, and chemical oxygen demand (COD) in ADLAM treatment attained by the IA-EI SBR process not only contributes to environmental preservation but also promotes the concepts of a circular economy. This process not only decreases the environmental impact of dairy operations, but also by transforming dairy effluent from contaminants to a potentially reusable resource. The integration of this process into existing dairy waste treatment systems implies a real step toward more sustainable, circular economy models in the dairy industry, supporting environmental sustainability and resource conservation.

3.3. Selection of optimal operating conditions for the IA-EI SBR using the Desirability function

To ascertain the optimal values of operating parameters for achieving the maximal removal efficiencies, the desirability function in the Design Expert software (version 13.0.5, Stat Ease, Inc., Minneapolis, MN, USA) was used to optimize multiple responses simultaneously. The operating parameters were kept "in range," while the goal for the responses was set at "maximize". The importance assigned to the five responses in the desirability approach were set at an equal level. The maximum desirability for the optimal set of conditions was 0.756 and the ideal operating conditions were 8 h of cycle time, 36 min/h of aeration time/strategy, 24 min of feed phases, and 100 min of idle phase. Under the optimal conditions, the optimal removal efficiencies of 82.64%, 95.82%, 92.92%, 73.84%, and 90.94% for $\%OP_{removal}$, $\%TP_{removal}$, $\%NH_3\text{-}N_{removal}$, $\%TN_{removal}$ and $\%COD_{removal}$, respectively (Table 5), were achieved during validation experiments. The validation experimental results were well within the ranges of 95% confidence interval (CI) predicted by the quadradic models**.** These results corroborate that IA-EI SBR process is an efficient and high performance in treating ADLDM and has potential to be scaled up as a real-world dairy wastewater treatment system. But further research is needed for systematic evaluation of the IA-EI SBR with continuous feeding schemes to estimate its adaptability in shifting influent conditions and energy demands. Also, the shift to this new system could require substantial infrastructural adjustments in existing dairy operations. It is critical to tackle these constraints in future research to safeguard the system's robustness and economic viability for large-scale application.

A comparison of the nutrient removal efficiencies between this study and previous investigations using SNDPR and DPR processes is summarized in Table 6. It is evident that, despite unfavorable influent characteristics, superior nutrient removal efficiencies were achieved in this study by optimizing the intermittent aeration time, feed, and idle phase durations. Table 6 suggests that SBR treating dairy wastewater were usually operated at higher HRTs than domestic or synthetic wastewater, due to the higher nutrient concentrations.

4. Conclusion

In this study, the potential application of a novel IA-EI SBR process for simultaneous removal P and N from ADLDM was thoroughly investigated by assessing the operating parameters, i.e., cycle time, aeration time, feed phases and idle phase. The optimal operating conditions were determined using CCD coupled with RSM. The quadratic models generated through CCD-RSM analysis based on the experimental results adequately predicted effects of operating parameters on the nutrient removal efficiencies (p-value ≤ 0.030). Results revealed that total phosphorus removal efficiency was significantly affected by the interactions of cycle time and idle phase (p-value $= 0.005$), and of the intermittent aeration strategy and feed phases (p-value $= 0.026$). Moreover, the efficiencies of total nitrogen ($\%TN_{removal}$) and COD ($\%COD_{removal}$) removals from ADLDM were significantly affected by interaction of intermittent aeration strategy and idle phase (p-value ≤ 0.006). Under the optimal operating conditions, viz, 8 h of cycle time, 36 min/h of aeration time, 24 min of two feed phases, and 100 min of idle phase, the statistically developed regression models predicted efficiencies of $\%OP_{removal}$, $\%TP_{removal}$, $\%NH_3\text{-}N_{removal}$, $\%TN_{removal}$ and $\%COD_{removal}$ at 84.26, 95.10, 91.90, 68.80, and 89.90%, respectively. Under 30 min/h aeration time and 7 h cycle with influent COD and TN loading of 3,999.2 and 785.7 mg.L^{-1}, the maximum SND efficiency of 85.7 % recorded. The efficiencies were validated experimentally with highly agreed values of 82.64, 95.82, 92.92, 73.84, and 90.94% for $\%OP_{removal}$, $\%TP_{removal}$, $\%NH_3\text{-}N_{removal}$,

TABLE 6 Enhanced N and P removal efficiencies using simultaneous nitrification-denitrification-P removal (SNDPR) or denitrifying P removal (DPR) processes in SBR.

Process classification and reactor	Waste streams	HRT (h)	DO concentration (mg L^{-1})	Inf C:N and Inf C:P ratio	Inf COD (mgL^{-1})	Inf N (mgL^{-1})	Inf P (mgL^{-1})	COD removal (%)	N removal (%)	*P* removal (%)	References
DPR in two-step fed IA-EI SBR	Anaerobically digested liquid dairy manure	72	$\leq$ 2.5	6:1 and 16: 1	4,083	720	261	90.9	73.8	95.8	This study
SNDPR process in two- step fed A_2O SBR	Dairy manure wastewater	72	–	6.8:1 and 78:1	6,970	1,013	89.2	95.6	97.9	97.6	Wu, 2017
SNDPR in low-O_2 granular SBR	Mixture of treated and raw cattle manure wastewater	32	0.3–1.0	9.1:1 and 145:1	11,000	1,198	76	79	99.9	97.7	Matinfar et al., 2019
DPR coupling with anammox and partial nitrification processes in anaerobic baffled reactor–membrane bioreactor	Domestic sewage wastewater	12.3	–	5.3:1 and 38: 1	284.6	52.7	7.5	88.3	61.9	54.4	Miao et al., 2020
2 L DPR reactor with 2 influent streams	Municipal Wastewater	9	$\leq$ 3	3.3:1 and 31:1	200	60	6.4	75.7	55.9	84.6	Liu et al., 2018
SNDPR in aerobic granular SBR	Synthetic wastewater	–	3–4	10.5:1 and 73:1	256.27	22	3.5	–	79.01	93.6	He et al., 2016
Nutrient removal in biofilm anaerobic fluidized bed reactor (AFBR)	real currant wastewater	18–48	–	11.6:1 and 46.2:1	462	40	10	93.0	84.0	68.0	Jaafari et al., 2014
N and P removal in A_2O biological aerated filter system	Domestic wastewater (adjusted with sodium acetate)	–	2 and 6	3:1 and 39:1, 5.5:1 and 71:1	220, 403	73.6, 73.2	5.6, 5.6	83.2, 90.3	66, 90	none	Chen et al., 2015

10.3389/fsufs.2023.1225792

$\%TN_{removal}$, and $\%COD_{removal}$ respectively. Based on the findings in this study, it can be proclaimed that the novel IA-EI SBR process established in this research can be a promising technology for removing nutrients from ADLDM with lower C: N and C: P ratios.

Data availability statement

The original contributions presented in the study are included in the article/Supplementary material, further inquiries can be directed to the corresponding author.

Author contributions

All authors listed have made a substantial, direct, and intellectual contribution to the work and approved it for publication.

Funding

This study was financially supported by the USDA National Institute of Food and Agriculture (NIFA) Hatch Project (Project No. IDA01604, Accession No. 1019082) and the USDA NIFA Sustainable Agricultural Systems project (Award No. 2020-69012-31871).

Acknowledgments

The authors wish to acknowledge Dr. Arif Reza and Kevin Kruger for their insights and assistance during the experiments.

Conflict of interest

The authors declare that the research was conducted in the absence of any commercial or financial relationships that could be construed as a potential conflict of interest.

Publisher's note

All claims expressed in this article are solely those of the authors and do not necessarily represent those of their affiliated organizations, or those of the publisher, the editors and the reviewers. Any product that may be evaluated in this article, or claim that may be made by its manufacturer, is not guaranteed or endorsed by the publisher.

Supplementary material

The Supplementary Material for this article can be found online at: https://www.frontiersin.org/articles/10.3389/fsufs.2023.1225792/full#supplementary-material

References

Albina, P., Durban, N., Bertron, A., Albrecht, A., Robinet, J. C., and Erable, B. (2019). Influence of hydrogen electron donor, alkaline ph, and high nitrate concentrations on microbial denitrification: a review. *Int. J. Mol. Sci.* 20, 5163. doi: 10.3390/ijms20205163

Anderson, M., and Whitcomb, P. (2017a). "Introduction to the Beauty of Response Surface Methods," in *RSM Simplified - Optimizing Processes Using Response Surface Methods for Design of Experiments*. Taylor and Francis Group. Available online at: https://www.routledge.com/RSM-Simplified-Optimizing-Processes-Using-Response-Surface-Methods-for/Anderson-Whitcomb/p/book/9781498745987 (accessed April 05, 2022).

Anderson, M. J., and Whitcomb, P. J. (2017b). *RSM simplified : Optimizing Processes Using Response Surface Methods for Design of Experiments*.

APHA, AWWA, and WEF. (2012). *Standard Methods for the Examination of Water and Wastewater* (Eugene W. Rice, Rodger, B. Baird, Andrew D. Eaton, and Lenore, S. Clesceri, Eds.; 22nd ed.). American Water Works Association.

Asghar, S., Chen, L., and He, B. (2023). Optimization of simultaneous nutrients and chemical oxygen demand removal from anaerobically digested liquid dairy manure in a two-step fed sequencing batch reactor system using taguchi method and grey relational analysis. *Appl. Biochemistr. Biotechnol.* 2023, 1–21. doi: 10.1007/s12010-023-04562-2

Barnard, J. L., Dunlap, P., and Steichen, M. (2017). Rethinking the mechanisms of biological phosphorus removal. *Water Environ. Res.* 89, 2043–2054. doi: 10.2175/106143017X15051465919010

Bassin, J. P., Kleerebezem, R., Dezotti, M., and van Loosdrecht, M. C. M. (2012). Simultaneous nitrogen and phosphate removal in aerobic granular sludge reactors operated at different temperatures. *Water Res.* 46, 3805–3816. doi: 10.1016/j.watres.2012.04.015

Bilici Baskan, M., and Pala, A. (2010). A statistical experiment design approach for arsenic removal by coagulation process using aluminum sulfate. *Desalination* 254, 42–48. doi: 10.1016/j.desal.2009.12.016

Caniani, D., Esposito, G., Gori, R., and Mannina, G. (2015). Towards a new decision support system for design, management and operation of wastewater treatment plants for the reduction of greenhouse gases emission. *Water* 7, 5599–5616. doi: 10.3390/w7105599

Carpenter, S. R., Caraco, N. F., Correll, D. L., Howarth, R. W., Sharpley, A. N., and Smith, V. H. (1998). Nonpoint pollution of surface waters with phosphorus and nitrogen. *Ecologic. Applicat.* 8, 559–568.

Castrillón, L., Fernández-Nava, Y., Marañón, E., García, L., and Berrueta, J. (2009). Anoxic–aerobic treatment of the liquid fraction of cattle manure. *Waste Manage.t* 29, 761–766. doi: 10.1016/j.wasman.2008.06.027

Chen, Y., Li, B., Ye, L., and Peng, Y. (2015). The combined effects of COD/N ratio and nitrate recycling ratio on nitrogen and phosphorus removal in anaerobic/anoxic/aerobic (A2/O)-biological aerated filter (BAF) systems. *Biochemic. Eng. J.* 93, 235–242. doi: 10.1016/j.bej.2014.10.005

Chen, Y., Peng, C., Wang, J., Ye, L., Zhang, L., and Peng, Y. (2011). Effect of nitrate recycling ratio on simultaneous biological nutrient removal in a novel anaerobic/anoxic/oxic (A2/O)-biological aerated filter (BAF) system. *Bioresour. Technol.* 102, 5722–5727. doi: 10.1016/j.biortech.2011.02.114

Cheng, Y., Li, J. Y., Ren, X., Li, Y., Kou, Y. Y., Chon, K., et al. (2022). High efficiency of simultaneous nitrification, denitrification, and organics removal in the real-scale treatment of high C/N ratio food-processing wastewater using micro-aerobic reactors. *Biochem. Eng. J.* 177, 108218. doi: 10.1016/j.bej.2021.108218

Dai, H., Han, T., Sun, T., Zhu, H., Wang, X., and Lu, X. (2021). Nitrous oxide emission during denitrifying phosphorus removal process: a review on the mechanisms and influencing factors. *J. Environ. Manag.* 278, 111561. doi: 10.1016/j.jenvman.2020.111561

Dai, H., Sun, Y., Wan, D., Abbasi, H. N., Guo, Z., Geng, H., et al. (2022). Simultaneous denitrification and phosphorus removal: a review on the functional strains and activated sludge processes. *Sci. Total Environ.* 835, 155409. doi: 10.1016/j.scitotenv.2022.155409

Dan, N. H., Rene, E. R., and le Luu, T. (2020). Removal of nutrients from anaerobically digested swine wastewater using an intermittent cycle extended aeration system. *Front. Microbiol.* 11, 38. doi: 10.3389/fmicb.2020.576438

Diez, M. C., Castillo, G., Aguilar, L., Vidal, G., and Mora, M. L. (2002). Operational factors and nutrient effects on activated sludge treatment of Pinus radiata kraft mill wastewater. *Bioresour. Technol.* 83, 131–138. doi: 10.1016/S0960-8524(01)00204-8

Dionisi, D., and Rasheed, A. A. (2018). Maximisation of the organic load rate and minimisation of oxygen consumption in aerobic biological wastewater treatment processes by manipulation of the hydraulic and solids residence time. *J. Water Process Eng.* 22, 138–146. doi: 10.1016/j.jwpe.2018.02.002

Fan, Z., Zeng, W., Liu, H., Jia, Y., and Peng, Y. (2022). A novel partial denitrification, anammox-biological phosphorus removal, fermentation and partial nitrification (PDA-PFPN) process for real domestic wastewater and waste activated sludge treatment. *Water Res.* 217, 118376. doi: 10.1016/j.watres.2022.118376

Ferrentino, R., Langone, M., Merzari, F., Tramonte, L., and Andreottola, G. (2016). "A review of anaerobic side-stream reactor for excess sludge reduction: Configurations, mechanisms, and efficiency," in *Critical Reviews in Environmental Science and Technology* ()London: Taylor and Francis Inc), 382–405.

Filip, D. S., and Middlebrooks, E. J. (1976). Eutrophication potential of dairy cattle waste runoff. *Water Res.* 10, 89–93. doi: 10.1016/0043-1354(76)90162-7

Guadie, A., Xia, S., Zhang, Z., Zeleke, J., Guo, W., Ngo, H. H., et al. (2014). Effect of intermittent aeration cycle on nutrient removal and microbial community in a fluidized bed reactor-membrane bioreactor combo system. *Bioresour. Technol.* 156, 195–205. doi: 10.1016/j.biortech.2014.01.008

Hai, R., He, Y., Wang, X., and Li, Y. (2015). Simultaneous removal of nitrogen and phosphorus from swine wastewater in a sequencing batch biofilm reactor. *Chinese J. Chem. Eng.* 23, 303–308. doi: 10.1016/j.cjche.2014.09.036

Hawkes, C., and Ruel, M. T. (2006). "Overview: understanding the links between agriculture and health," in *2020 Vision Briefs*. Available online at: https://ideas.repec.org/p/fpr/2020br/13(1).html doi: 10.2499/Focus13CH1

He, Q., Song, J., Zhang, W., Gao, S., Wang, H., and Yu, J. (2020). Enhanced simultaneous nitrification, denitrification and phosphorus removal through mixed carbon source by aerobic granular sludge. *J. Hazard. Mater.* 382, 782. doi: 10.1016/j.jhazmat.2019.121782

He, Q., Zhang, S., Zou, Z., Zheng, L., an, and Wang, H. (2016). Unraveling characteristics of simultaneous nitrification, denitrification and phosphorus removal (SNDPR) in an aerobic granular sequencing batch reactor. *Bioresour. Technol.* 220, 651–655. doi: 10.1016/j.biortech.2016.08.105

Izadi, P., Izadi, P., and Eldyasti, A. (2021). Enhancement of simultaneous nitrogen and phosphorus removal using intermittent aeration mechanism. *J. Environ. Sci.* 109, 1–14. doi: 10.1016/j.jes.2021.02.026

Jaafari, J., Mesdaghinia, A., Nabizadeh, R., Hoseini, M., Kamani, H., and Mahvi, A. H. (2014). Influence of upflow velocity on performance and biofilm characteristics of Anaerobic Fluidized Bed Reactor (AFBR) in treating high-strength wastewater. *J. Environ. Health Sci. Eng.* 12, 1–10. doi: 10.1186/s40201-014-0139-x

Ji, J., Peng, Y., Wang, B., Li, X., and Zhang, Q. (2020). A novel SNPR process for advanced nitrogen and phosphorus removal from mainstream wastewater based on anammox, endogenous partial-denitrification and denitrifying dephosphatation. *Water Res.* 170, 115363. doi: 10.1016/j.watres.2019.115363

Kargi, F., and Uygur, A. (2003). Effect of carbon source on biological nutrient removal in a sequencing batch reactor. *Bioresour. Technol.* 89, 89–93. doi: 10.1016/S0960-8524(03)00031-2

Kuba, T., van Loosdrecht, M. C. M., and Heijnen, J. J. (1996). Phosphorus and nitrogen removal with minimal COD requirement by integration of denitrifying dephosphatation and nitrification in a two-sludge system. *Water Res.* 30, 1702–1710. doi: 10.1016/0043-1354(96)00050-4

Lee, H., Brereton, J. A., Mavinic, D. S., Fiorante, R. A., Oldham, W. K., and Paisley, J. K. (2001). Nutrient removal with methanol as a carbon source full-scale continuous inflow SBR application. *Environ. Technol.* 22, 1223–1235. doi: 10.1080/09593332208618208

Leonard, P., Tarpey, E., Finnegan, W., and Zhan, X. (2018). Efficient treatment of dairy processing wastewater in a laboratory scale Intermittently Aerated Sequencing Batch Reactor (IASBR). *Journal of Dairy Research* 85, 379–383. doi: 10.1017/S0022029918000584

Li, C., Liu, S., Ma, T., Zheng, M., and Ni, J. (2019). Simultaneous nitrification, denitrification and phosphorus removal in a sequencing batch reactor (SBR) under low temperature. *Chemosphere* 229, 132–141. doi: 10.1016/j.chemosphere.2019.04.185

Li, P., Zuo, J., Wang, Y., Zhao, J., Tang, L., and Li, Z. (2016). Tertiary nitrogen removal for municipal wastewater using a solid-phase denitrifying biofilter with polycaprolactone as the carbon source and filtration medium. *Water Res.* 93, 74–83. doi: 10.1016/j.watres.2016.02.009

Liu, H., Yao, Y., and Xu, S. (2018). Removal and transformation of pollutants in a two-line denitrifying phosphorus removal process treating low C/N municipal wastewater: influence of hydraulic retention time. *Water Air Soil Pollut.* 229, 1–9. doi: 10.1007/s11270-018-3746-9

Liu, T., Liu, S., He, S., Tian, Z., and Zheng, M. (2021). Minimization of N2O emission through intermittent aeration in a sequencing batch reactor (sbr): main behavior and mechanism. *Water* 13, 210. doi: 10.3390/w13020210

Lochmatter, S., Gonzalez-Gil, G., and Holliger, C. (2013). Optimized aeration strategies for nitrogen and phosphorus removal with aerobic granular sludge. *Water Res.* 47, 6187–6197. doi: 10.1016/j.watres.2013.07.030

Louzeiro, N. R., Mavinic, D. S., Oldham, W. K., Meisen, A., and Gardner, I. S. (2002). Methanol-induced biological nutrient removal kinetics in a full-scale sequencing batch reactor. *Water Res.* 36, 2721–2732. doi: 10.1016/S0043-1354(01)00494-8

Mang, N. Z. L., Hwang, Y., and Lee, T.-J. (2022). Optimization of the step feeding ratio for nitrogen removal by SBR using technique for order preference by similarity to ideal solution (TOPSIS). *Environ. Eng. Res.* 27, 200685–200680. doi: 10.4491/eer.2020.685

Marañón, E., Castrillón, L., García, L., Vázquez, I., and Fernández-Nava, Y. (2008). Three-step biological process for the treatment of the liquid fraction of cattle manure. *Bioresource Technol.* 99, 7750–7757. doi: 10.1016/j.biortech.2008.01.065

Matinfar, A., Mohammadi, M., Najafpour, G. D., and Younesi, H. (2019). Ammonia and phosphorus removal from mixture of treated and raw cattle manure wastewater in a low-O2 granular sequencing batch reactor. *J. Chem. Technol. Biotechnol.* 94, 2238–2247. doi: 10.1002/jctb.6011

Miao, X. N., Wang, Q., Guo, K. C., Liu, W. R., and Shen, Y. L. (2020). Start-up and Optimization of Denitrifying Phosphorus Removal in ABR-MBR Coupling Process. *Huan Jing Ke Xue = Huanjing Kexue* 41, 4150–4160.

New Patented Technology Removes Phosphorus from Manure (2018). *Pennsylvania State University*. Available online at: https://phys.org/news/2018-04-patented-technology-phosphorus-manure.html (accessed April 9, 2018).

Raper, E., Fisher, R., Anderson, D. R., Stephenson, T., and Soares, A. (2018). Alkalinity and external carbon requirements for denitrification-nitrification of coke. *Wastewater*. 39, 2266–2277. doi: 10.1080/09593330.2018.1437779

Rollemberg, S. L., de, S., de Oliveira, L. Q., Barros, A. R. M., Melo, V. M. M., Firmino, P. I. M., et al. (2019). Effects of carbon source on the formation, stability, bioactivity and biodiversity of the aerobic granule sludge. *Bioresour. Technol.* 278, 195–204. doi: 10.1016/j.biortech.2019.01.071

Shen, Y., Yang, D., Wu, Y., Zhang, H., and Zhang, X. (2019). Operation mode of a step-feed anoxic/oxic process with distribution of carbon source from anaerobic zone on nutrient removal and microbial properties. *Scientific Rep.* 9, 1–11. doi: 10.1038/s41598-018-37841-8

The Issue | US EPA. (n.d.). Retrieved 6 April 2022, from https://www.epa.gov/nutrientpollution/issue (accessed August 11, 2022).

Understanding Global Warming Potentials | US EPA (2022). *United State Environmental Protection Agency*. Available online at: https://www.epa.gov/ghgemissions/understanding-global-warming-potentials (accessed May 5, 2022).

Wang, D., bo, Li, X., ming, Yang, Q., Zeng, G., ming, Liao, D., xiang, and Zhang, J. (2008). Biological phosphorus removal in sequencing batch reactor with single-stage oxic process. *Bioresour. Technol.* 99, 5466–5473. doi: 10.1016/j.biortech.2007.11.007

Wang, D., Li, X., Yang, Q., Zheng, W., Wu, Y., Zeng, T., et al. (2012). Improved biological phosphorus removal performance driven by the aerobic/extended-idle regime with propionate as the sole carbon source. *Water Res.* 46, 3868–3878. doi: 10.1016/j.watres.2012.04.036

Wang, H., Song, Q., Wang, J., Zhang, H., He, Q., Zhang, W., et al. (2018). Simultaneous nitrification, denitrification and phosphorus removal in an aerobic granular sludge sequencing batch reactor with high dissolved oxygen: Effects of carbon to nitrogen ratios. *Sci. Total Environ.* 642, 1145–1152. doi: 10.1016/j.scitotenv.2018.06.081

Wang, L., Chen, L., and Wu, S. (2020a). Nutrient reduction of dairy manure through solid-liquid separation with flocculation and subsequent microalgal treatment. *Appl. Biochemistr. Biotechnol.* 190, 1425–1437. doi: 10.1007/s12010-019-03185-w

Wang, L., Chen, L., and Wu, S. (2020b). Microalgae cultivation using screened liquid dairy manure applying different folds of dilution: nutrient reduction analysis with emphasis on phosphorus removal. *Appl. Biochemistr. Biotechnol.* 192, 381–391. doi: 10.1007/s12010-020-03316-8

Wang, Y., Peng, Y., and Stephenson, T. (2009). Effect of influent nutrient ratios and hydraulic retention time (HRT) on simultaneous phosphorus and nitrogen removal in a two-sludge sequencing batch reactor process. *Bioresour. Technol.* 100, 26. doi: 10.1016/j.biortech.2009.02.026

Wu, S. (2017). Nutrient removal and nitrous oxide emission by a two-step fed sbr in treating dairy manure wastewater. *Transact. ASABE* 60, 1729–1736. doi: 10.13031/trans.12411

Wu, T., Yang, S. S., Zhong, L., Pang, J. W., Zhang, L., Xia, X. F., et al. (2023). Simultaneous nitrification, denitrification and phosphorus removal: What have we done so far and how do we need to do in the future? *Sci. Total Environ.* 856, 158977. doi: 10.1016/j.scitotenv.2022.158977

Wu, X., Zhu, J., Cheng, J., and Zhu, N. (2015). Optimization of three operating parameters for a two-step fed sequencing batch reactor (sbr) system to remove nutrients from swine wastewater. *Appl. Biochemistr. Biotechnol.* 175, 2857–2871. doi: 10.1007/s12010-014-1467-0

Yoo, H., Ahn, K.-. H., Lee, H.-. J., Lee, K.-. H., Kwak, Y.-. J., et al. (1999). Nitrogen removal from synthetic wastewater by simultaneous nitrification and denitrification (SND) via nitrite in an intermittently-aerated reactor. *Water Res.* 33, 6. doi: 10.1016/S0043-1354(98)00159-6

Yuan, C., Wang, B., Peng, Y., Li, X., Zhang, Q., and Hu, T. (2020). Enhanced nutrient removal of simultaneous partial nitrification, denitrification and phosphorus removal (SPNDPR) in a single-stage anaerobic/micro-aerobic sequencing batch reactor for treating real sewage with low carbon/nitrogen. *Chemosphere* 257, 127097. doi: 10.1016/j.chemosphere.2020.127097

Zeng, R. J., Lemaire, R., Yuan, Z., and Keller, J. (2003). Simultaneous nitrification, denitrification, and phosphorus removal in a lab-scale sequencing batch reactor. *Biotechnol. Bioeng.* 84, 170–178. doi: 10.1002/bit.10744

Zhang, L., Zhang, S., Wang, S., Wu, C., Chen, Y., Wang, Y., et al. (2013). Enhanced biological nutrient removal in a simultaneous fermentation, denitrification and phosphate removal reactor using primary sludge as internal carbon source. *Chemosphere* 91, 635–640. doi: 10.1016/j.chemosphere.2012.12.071

Zhang, M., Gao, J., Fan, Y., Wu, X., Wu, J., and He, C. (2021). Combined effects of volume ratio and nitrate recycling ratio on nutrient removal, sludge characteristic and microbial evolution for DPR optimization. *J. Environ. Sci.* 104, 69–83. doi: 10.1016/j.jes.2020.12.003

Zhang, M., Qiao, S., Shao, D., Jin, R., and Zhou, J. (2018). Simultaneous nitrogen and phosphorus removal by combined anammox and denitrifying phosphorus removal process. *J. Chem. Technol. Biotechnol.*, 93, 94–104. doi: 10.1002/jctb.5326

Zhang, M., Wan, J., Fan, Y., Yong, D., Liu, Y., Ji, J., et al. (2022). Bioaugmentation for low C/N ratio wastewater treatment by combining endogenous partial denitrification (EPD) and denitrifying phosphorous removal (DPR) in the continuous A2/O - MBBR system. *J. Environ. Manag.* 312, 114920. doi: 10.1016/j.jenvman.2022.114920

Zhang, X., Wang, C., Wu, P., Xia, Y., Chen, Y., Liu, W., et al. (2021). A novel denitrifying phosphorus removal and partial nitrification, anammox (DPR-PNA) process for advanced nutrients removal from high-strength wastewater. *Chemosphere* 265, 129165. doi: 10.1016/j.chemosphere.2020.129165